JACS
JOURNAL OF THE AMERICAN CHEMICAL SOCIETY

COMMUNICATION

pubs.acs.org/JACS

4D Scanning Transmission Ultrafast Electron Microscopy: Single-Particle Imaging and Spectroscopy

Volkan Ortalan and Ahmed H. Zewail*

Physical Biology Center for Ultrafast Science and Technology, Arthur Amos Noyes Laboratory of Chemical Physics, California Institute of Technology, Pasadena, California 91125, United States

Web-Enhanced

ABSTRACT: We report the development of 4D scanning transmission ultrafast electron microscopy (ST-UEM). The method was demonstrated in the imaging of silver nanowires and gold nanoparticles. For the wire, the mechanical motion and shape morphological dynamics were imaged, and from the images we obtained the resonance frequency and the dephasing time of the motion. Moreover, we demonstrate here the simultaneous acquisition of dark-field images and electron energy loss spectra from a single gold nanoparticle, which is not possible with conventional methods. The local probing capabilities of ST-UEM open new avenues for probing dynamic processes, from single isolated to embedded nanostructures, without being affected by the heterogeneous processes of ensemble-averaged dynamics. Such methodology promises to have wide-ranging applications in materials science and in single-particle biological imaging.

The development of ultrafast electron microscopy (UEM) has enabled studies of structural dynamics in both space and time with atomic-scale resolution.[1,2] With UEM, different techniques of electron microscopy[3] were made possible with femtosecond time resolution: real-space imaging,[4,5] diffraction,[6−8] tomography,[9] near-field electron microscopy,[10] and electron energy loss spectroscopy (EELS).[11,12] In all of these varients, UEM utilizes electron beams for parallel illumination in imaging and for EELS; in convergent beam studies, diffraction was recorded in order to obtain the dynamics.[8] Scanning transmission electron microscopy (STEM) provides unique advantage for imaging.[13,14] Utilizing high angle scatterings, which lead to strong atomic number (Z^2)-dependent contrast (incoherent imaging), enables a straightforward interpretation of the image.[15] Moreover, localized nanoscale regions of a sample can be imaged while simultaneously collecting an EEL spectrum from that particular region.[16,17]

In this Communication, we report the development of 4D scanning transmission ultrafast electron microscopy (ST-UEM). Applications of ST-UEM are demonstrated for nanostructured materials, i.e., silver nanowires and gold nanoparticles, with the time resolution being independent of the video camera response time (milliseconds), thus enabling the visualization of dynamical processes on the femtosecond to millisecond time scales. For the silver nanowire, the ST-UEM movie displays the mechanical motion and shape morphological dynamics of the cantilever-type object, following an impulsive heating, and directly from the image frames we obtained the natural frequency and the damping (dephasing) rate of the mechanical vibration involved. For a single gold nanoparticle, ultrafast simultaneous imaging in the dark- and bright-field modes together with the associated EEL spectra was obtained for the first time.

Shown in Figure 1 is a schematic depiction of the ST-UEM methodology. A dark-field image is formed by scanning a convergent electron probe pulse across a specimen in a raster fashion while collecting the high-angle transmitted, elastically scattered electrons via an annular detector located below the specimen. Additionally, the transmitted electrons that pass through the hole in the annular detector can be utilized to form bright-field images (elastically scattered electrons) or to provide an EEL spectrum (inelastically scattered electrons). In this configuration, we recorded the image frames at different times of the probed sample area together with the EEL spectrum having information on chemical bonding dynamics, electronic structural changes, structural dynamics, etc.[11,12,18] Because of the small size of the convergent electron probe pulse, the effect of the inhomogeneity, such as defects and interfaces, which determines materials' electronic, optical, and magnetic properties, can be mapped out by investigating the local dynamics and the variations across the specimen, from nanometers to micrometers.

In these studies, two laser systems were invoked, depending on the time scale of interest. The investigations on silver nanowires and gold nanoparticles have been performed using nanosecond and femtosecond lasers, respectively. The structural change was initiated utilizing a heat pulse, and the images were recorded using the optically generated electron pulse.[7,19,20] The timing was controlled by changing the delay time of the electron pulse (probing) with respect to the initiating pulse (pump), either electronically in the nanosecond mode or optically (delay stage) in the femtosecond mode. The electrons were accelerated to 200 kV, giving a de Broglie wavelength of 2.5 pm. The image construction is achieved through the scanning process of the electron probe pulse with well-defined dwell time for each position of the probe. There is a direct correspondence between the location of the electron probe on the specimen and the pixels forming the images.

In Figure 2, we present time-resolved dark-field ST-UEM images of a silver nanowire for two representative time frames. Each time frame was constructed stroboscopically from multiple

Received: April 26, 2011
Published: May 26, 2011

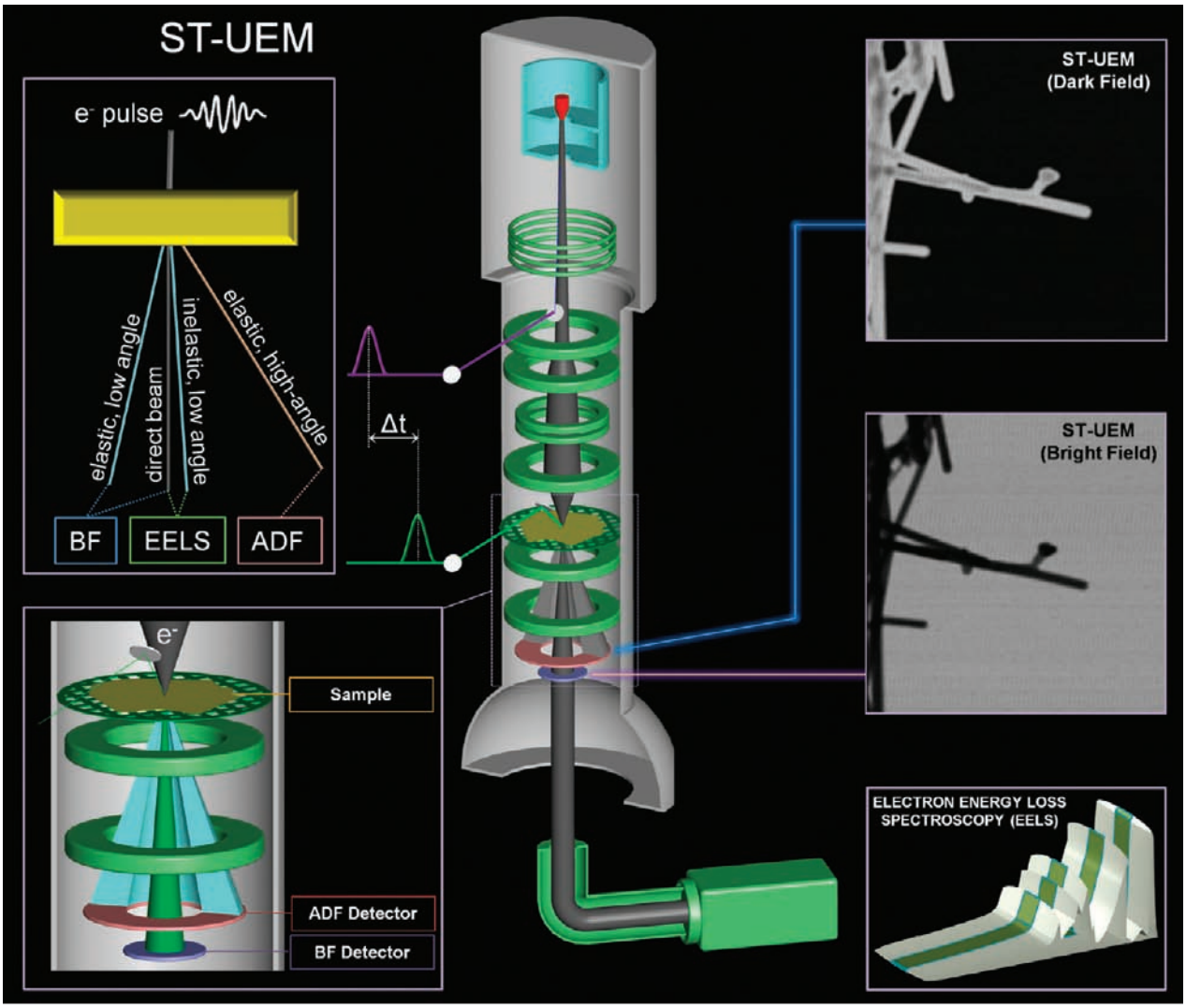

Figure 1. Scanning transmission ultrafast electron microscopy (ST-UEM). Left: illustration of electron-specimen interaction and the expected scatterings that lead to bright-field (BF), annular dark-field (ADF), and EELS recordings. Right, from top to bottom: ST-UEM dark-field image frame of the cantilever-type nanostructure obtained utilizing the ADF mode and ST-UEM bright-field image using the BF mode. The inelastically scattered electrons are collected by the electron energy loss spectrometer. The time delay, Δt, between the probe electron pulse and the pump laser pulse is indicated in the conceptual schematic of ST-UEM (center).

images. In this way the image intensity fluctuations are suppressed and the signal-to-noise is optimized. At positive times, after the initiating pulse, visual changes are clear in the image. A movie formed from the frames illustrates the mechanical motion of the silver nanowire following the heating pulse, and the motion is clearly resolved (movie S1). There is no noticeable change in the images collected before the arrival of the heating pulse, i.e., after the exposure to electron pulses at positive time, indicating that the system recovers to its original structure in less than 100 μs. Moreover, there is no observable difference for the images collected at a fixed time delay, which were used to build up the frame, and this would not be possible if the structure was not completely back to its original state. There was no sign of plastic deformation of the nanowire during these experiments.

The plot in Figure 2 illustrates the change in the projected length of the silver nanowire with time, which exhibits a damped oscillatory behavior. The projected length data have been fitted to an exponentially decaying sinusoidal function: $L = A\sin(wt + \varphi)\exp(-kt) + c$, where k is the damping rate constant, w is the frequency, and c is a constant. The period gives a resonance frequency of ~0.4 MHz. The damping time of the motion can be estimated; in this case, the results indicate that the mechanical vibration dies out in about 60 μs.

In order to examine single-particle imaging feasibility, we used the dark- and bright-field imaging of the femtosecond ST-UEM (Figure 3). The bright-field detector (Figure 1) records the transmitted beam, and therefore the "vacuum" appears bright, whereas the ADF detector excludes the transmitted beam, and the "vacuum" appears dark. The DF ST-UEM image is more sensitive to high-Z elements and, therefore, provides a high degree of chemical information. On the other hand, the main advantage of the BF ST-UEM image is that it is more sensitive to light atoms. As is evident from the images in Figure 3, the simultaneous recording of DF and BF frames is advantageous; while the amorphous carbon (low-Z) film supporting the gold nanoparticle is not visible in the DF ST-UEM image, the BF image clearly shows the amorphous carbon substrate.

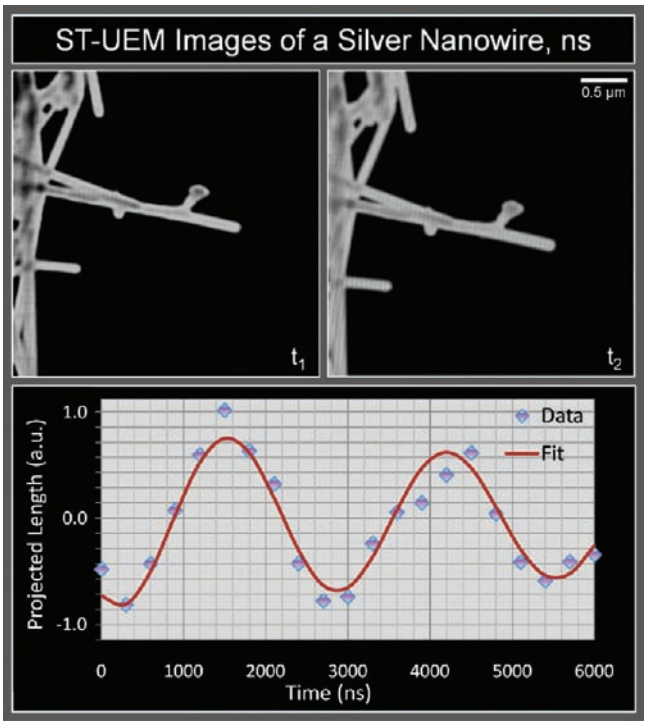

Figure 2. Dynamic ST-UEM DF images of a silver nanowire. For the mechanical motion, snapshots of images are given for two relevant -to-the motion time delays, t_1 = 30 ns and t_2 = 2400 ns. The motion from the time-dependent projected length of the nanowire displays the oscillatory motion shown at the bottoms, and for this structure the fit gives a resonance frequency of ~0.4 MHz; it damps in ~60 μs. The different frames taken show the mechanical vibration of the cantilever projected in the image (see movie S1).

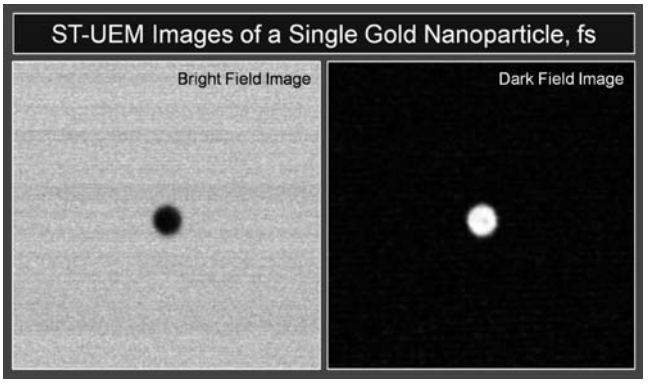

Figure 3. Femtosecond dark- and bright-field ST-UEM images obtained simultaneously for a single gold nanoparticle. The "vacuum" appears dark in the dark-field images and bright in the bright-field images. The gold nanoparticle with spherically symmetric shape is supported on an amorphous carbon film. The low-atomic carbon film is more visible in the bright-field ST-UEM image. Image processing is similar to that used for Figure 2. The particle size varies, and in this case it is close to 140 nm.

One of the most important advantages of ST-UEM is the ability to collect simultaneously images and EEL spectra from a local nanosize area without effect from the rest of the sample. In our ST-UEM, which is equipped with an EEL spectrometer, it is

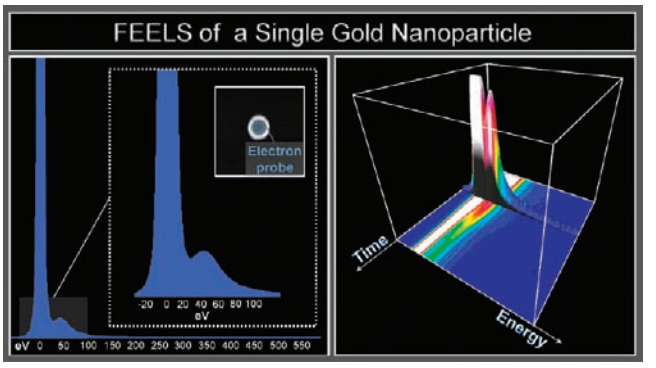

Figure 4. Femtosecond electron energy loss spectra (FEELS) of a single gold nanoparticle in the ST-UEM mode. The convergent electron probe pulse in ST-UEM allows us to collect the spectra of a single gold nanoparticle. Shown is one frame of the spectra obtained with femtosecond resolution and displays the zero loss and the plasmon peaks, which are important for probing the dynamics of acoustic vibrations (see text). The projected contour in energy—time space describes the possible FEELS mapping of change in dynamics.

possible to probe plasmon resonances in metal nanoparticles with femtosecond time and nanometer spatial resolution. The plasmon peaks are in the low loss region of the EEL spectrum (<100 eV) and have a relatively high intensity. Accordingly, shifts in the plasmon peaks are particularly suitable for probing the acoustic vibrations of nanostructures. Figure 4A illustrates such an EEL spectrum collected from a single gold nanoparticle in which the vibrations are excited by an ultrafast pump laser pulse. By changing the time delay between the initiating pump and the probe (electron) pulse, it was possible to obtain a time-resolved femtosecond EEL spectrum surface, as depicted in Figure 4B.

The above resolutions in image and energy domains cannot be obtained from optical studies of heterogeneous specimens. This is because the properties of nanostructures strongly depend on their individual size and shape.[21] The spatial resolution of optical spectroscopy on the micrometer scale limits the applicability of the technique to the study of heterogeneous samples, necessitating the use of extremely high quality samples with narrow size/shape distribution. Synthesis of such a structure is a daunting challenge. Moreover, neither optical spectroscopy nor electron microscopy with parallel illumination can be applied to the phase-separated embedded nanostructures within another matrix material, interfaces, and defects. The nanometer-sized (and below) convergent electron beam of ST-UEM provides the mean to selectively investigate dynamic processes in heterogeneous samples; examples include the coherent excitation of vibrational modes in nanoparticles[22] and the breathing motion of a local catalytic site.[23]

In conclusion, with 4D ST-UEM, we demonstrated here time-resolved imaging (dark and bright field) of a single particle, spherical or shaped, by utilizing convergent electron pulses and EEL spectra from the probed particles. The methodology is wide ranging in applications, particularly in heterogeneous systems, because incoherent imaging (Z^2 dependence) makes visualization specific to component elements and to the selected area. Unlike scanning ultrafast electron microscopy (SUEM),[24,25] ST-UEM operates in the transmission mode, providing atomic-scale resolution in the image and permitting direct information

on EELS for the analytical signature of the specimen.[26,27] Future applications can now make use of the full space-time range of ST-UEM in single-particle and tomographic imaging of materials and biological structures.

Web Enhanced Feature. Movie S1 (.avi) formed from the frames obtained during time-resolved dark-field ST-UEM, illustrating the mechanical motion of a silver nanowire following the heating pulse, is available in the HTML version.

AUTHOR INFORMATION

Corresponding Author
zewail@caltech.edu

ACKNOWLEDGMENT

A.H.Z. acknowledges the helpful discussion with Prof. Archie Howie regarding STEM. This work was supported by National Science Foundation Grant DMR-0964886 and Air Force Office of Scientific Research Grant FA9550-07-1-0484 in Caltech's Physical Biology Center for Ultrafast Science and Technology, supported by the Gordon and Betty Moore Foundation.

REFERENCES

(1) Zewail, A. H. *Science* **2010**, *328*, 187.
(2) Zewail, A. H.; Lobastov, V. U.S. Patent 7,154,091 B2, 20050401, 2006.
(3) Thomas, J. M.; Midgley, P. *Chem. Phys.* **2011**, 381.
(4) Park, H. S.; Baskin, J. S.; Kwon, O. H.; Zewail, A. H. *Nano Lett.* **2007**, *7*, 2545.
(5) Kwon, O. H.; Barwick, B.; Park, H. S.; Baskin, J. S.; Zewail, A. H. *Nano Lett.* **2008**, *8*, 3557.
(6) Grinolds, M. S.; Lobastov, V. A.; Weissenrieder, J.; Zewail, A. H. *Proc. Natl. Acad. Sci. U.S.A.* **2006**, *103*, 18427.
(7) Barwick, B.; Park, H. S.; Kwon, O. H.; Baskin, J. S.; Zewail, A. H. *Science* **2008**, *322*, 1227.
(8) Yurtsever, A.; Zewail, A. H. *Science* **2009**, *326*, 708.
(9) Kwon, O. H.; Zewail, A. H. *Science* **2010**, *328*, 1668.
(10) Barwick, B.; Flannigan, D. J.; Zewail, A. H. *Nature* **2009**, *462*, 902.
(11) Carbone, F.; Kwon, O. H.; Zewail, A. H. *Science* **2009**, *325*, 181.
(12) Thomas, J. M. *Angew. Chem., Int. Ed.* **2009**, *48*, 8824.
(13) Crewe, A. V.; Wall, J.; Langmore, J. *Science* **1970**, *168*, 1338.
(14) Midgley, P. A.; Weyland, M.; Yates, T. J. V.; Arslan, I.; Dunin-Borkowski, R. E.; Thomas, J. M. *J. Microsc.* **2006**, *223*, 185.
(15) Hartel, P.; Rose, H.; Dinges, C. *Ultramicroscopy* **1996**, *63*, 93.
(16) Muller, D. A.; Mills, M. J. *Mater. Sci. Eng., A* **1999**, *260*, 12.
(17) Pennycook, S. J.; Jesson, D. E.; McGibbon, A. J.; Nellist, P. D. *J. Electron Microsc.* **1996**, *45*, 36.
(18) Egerton, R. F. *Electron Energy-Loss Spectroscopy in the Electron Microscope*; Plenum Press: New York, 1996.
(19) Zewail, A. H., Thomas, J. M. *4D Electron Microscopy: Imaging in Space and Time*; Imperial College Press: London, 2010.
(20) Park, H. S.; Baskin, J. S.; Kwon, O. H.; Zewail, A. H. *Nano Lett.* **2007**, *7*, 2545.
(21) Koh, A. L.; Bao, K.; Khan, I.; Smith, W. E.; Kothleitner, G.; Nordlander, P.; Maier, S. A.; McComb, D. W. *ACS Nano* **2009**, *3*, 3015.
(22) Hartland, G. V. *Phys. Chem. Chem. Phys.* **2004**, *6*, 5263.
(23) Thomas, J. M.; Catlow, C. R. A.; Sankar, G. *Chem. Commun.* **2002**, *24*, 2921.
(24) Yang, D. S.; Mohammed, O. F.; Zewail, A. H. *Proc. Natl. Acad. Sci. U.S.A.* **2010**, *107*, 14993.
(25) Mohammed, O. F.; Yang, D. S.; Pal, S. K.; Zewail, A. H. *J. Am. Chem. Soc.* **2011**, *133*, 7708.
(26) Muller, D. A.; Kourkoutis, L. F.; Murfitt, M.; Song, J. H.; Hwang, H. Y.; Silcox, J.; Dellby, N.; Krivanek, O. L. *Science* **2008**, *319*, 1073.
(27) Krivanek, O. L.; Chisholm, M. F.; Nicolosi, V.; Pennycook, T. J.; Corbin, G. J.; Dellby, N.; Murfitt, M. F.; Own, C. S.; Szilagyi, Z. S.; Oxley, M. P.; Pantelides, S. T.; Pennycook, S. J. *Nature* **2010**, *464*, 571.